Application of Curved Parametric Triangular and Quadrilateral Edge Elements in the Moment Method Solution of the EFIE

Ning Yan Zhu, *Member, IEEE,*, and Friedrich M. Landstorfer, *Senior Member, IEEE*

Abstract— **The application is reported of curved parametric triangular and quadrilateral edge elements, which have been successfully applied in the finite-element method (FEM) in the last 10 years, as basis functions in the moment method (MM) solution of the electric field integral equation (EFIE). In this way, an arbitrarily shaped surface can be modeled more accurately than with conventional planar patches. Consequently, higher accuracy in the numerical solution can mostly be obtained, as demonstrated by numerical examples.**

I. Introduction

IN THE classical papers on the MM solution of the EFIE for electromagnetic scattering from perfectly conducting surfaces of arbitrary shape ([1], [2]), the importance of the continuity of the normal current components across the boundary of a patch in the basis functions has been pointed out, and basis functions which fulfil this requirement have been introduced for planar rectangular and triangular patches. Since then, due to their ability of modeling general geometrical shapes, these basis functions, especially the ones for planar triangular patches, have found wide application.

For modeling an *arbitrary* surface, many planar triangular patches may be necessary, however. As a remedy, curved parametric patches could be used instead. Actually, as early as 1972, curved parametric quadrilaterals with 9 nodes were used to model a given surface together with piecewise constant basis functions in the MM solution of the magnetic field integral equation (MFIE) [3]. Recently, new results using curved parametric patches in the MFIE are reported (e.g., [4], [5]). There interpolation functions of the unknown current values at nodal points are chosen as basis functions. The associated difficulties for currents at sharp geometric edges can be avoided by using "semidiscontinuous boundary elements" [4].

On the other hand, a new class of basis functions, i.e., edge elements, appeared in the FEM in last decade. In these elements, the unkowns are no longer the field values at nodal points, but their integrals along the element edges. On the element boundaries, only the continuity of the tangential field components is enforced. With this kind of elements the nonphysical solutions in the FEM associated with nodal based elements can completely be eliminated (e.g., [6]).

Manuscript received May 17, 1993. This work was supported in part by Deutsche Forschungsgemeinschaft (DFG) under La 484/2-2 and La 484/8-1.

The authors are with the Institut für Hochfrequenztechnik, Universität Stuttgart, Pfaffenwaldring 47, 70 550 Stuttgart, Germany.

IEEE Log Number 9211890.

In appreciation of this, a direct and systematic application of first-order edge elements, combined with a quadratic parametric description of the patch geometry, in the MM solution of the EFIE as basis functions, is the subject of this letter. For the sake of completeness, it should be mentioned that basis functions for curved parametric *triangular* patches have been proposed recently ([7], [8]), but from a different point of view and vectorial finite elements for curved triangles were reported in [9].

II. Basis Functions

A. Curved Parametric Triangles

A quadratic parametric triangle is uniquely determined by its six nodal points $\boldsymbol{r}_i$ $(i = 1, \cdots, 6)$ together with its corresponding interpolation functions $N_i(\xi_1, \xi_2, \xi_3)$. ξ_j $(1 \le j \le 3)$ are the area–coordinates with $\sum_j \xi_j = 1$ and $0 \le \xi_j \le 1$ [10]. Hence, each point $\boldsymbol{r}(\xi_1, \xi_2, \xi_3)$ on this triangle can be represented by $\boldsymbol{r}(\xi_1, \xi_2, \xi_3) = \sum_{i=1}^{6} \boldsymbol{r}_i N_i(\xi_1, \xi_2, \xi_3)$.

It is assumed that the basis function $\boldsymbol{W}_{ij}$ associated with edge ij, which connects nodes i and j, for the magnetic field intensity is given by (e.g., [6]): $\boldsymbol{W}_{ij} = \xi_i \,\mathrm{grad}\xi_j - \xi_j \,\mathrm{grad}\xi_i$. It can be shown that $\boldsymbol{W}_{ij}$ is orthogonal to the other two edges.

With $\boldsymbol{r}_{\xi_j} = \partial \boldsymbol{r}/\partial \xi_j$ the normal vector $\boldsymbol{n}$ of this surface is defined by $\boldsymbol{n} = \boldsymbol{r}_{\xi_i} \times \boldsymbol{r}_{\xi_j}/|\boldsymbol{r}_{\xi_i} \times \boldsymbol{r}_{\xi_j}|$. The basis function $\boldsymbol{B}_{ij}$ associated with edge ij for the current distributions on the surface can then easily be derived:

$$\boldsymbol{B}_{ij} = \boldsymbol{n} \times \boldsymbol{W}_{ij} = -(\xi_i \boldsymbol{r}_{\xi_i} + \xi_j \boldsymbol{r}_{\xi_j})/|\boldsymbol{r}_{\xi_i} \times \boldsymbol{r}_{\xi_j}|. \quad (1)$$

In the derivation use is made of the well-known relation $\boldsymbol{r}_{\xi_i} \cdot \,\mathrm{grad}\xi_j = \delta_{ij}$, where δ_{ij} is Kronecker symbol. $\boldsymbol{B}_{ij}$ is parallel to the other two edges (Fig. 1(a)). Additionally, a useful equation for basis functions previously derived is given by $\mathrm{div}_S \boldsymbol{B}_{ij} = -2/|\boldsymbol{r}_{\xi_i} \times \boldsymbol{r}_{\xi_j}|$, where div_S means surface divergence.

B. Curved Parametric Quadrilaterals

The basis functions for the current distributions on a curved parametric quadrilateral can be derived in the same way as for triangles from the corresponding edge elements. The latter have been taken from [11]. The results are given next.

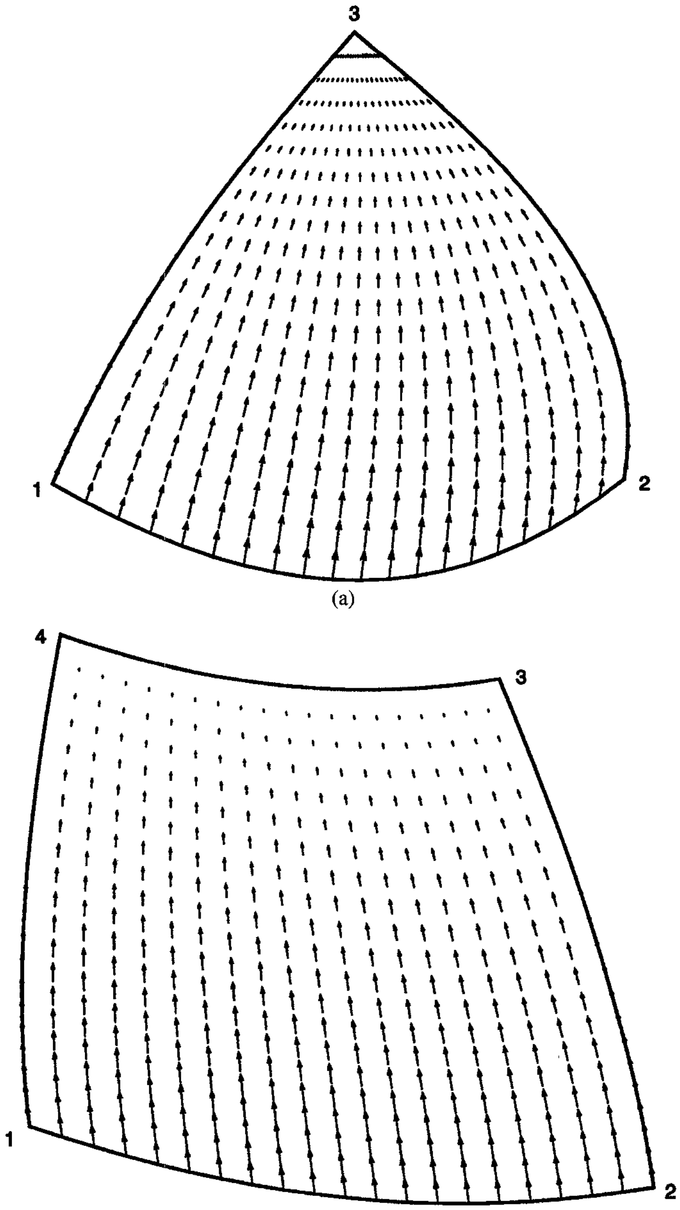

(a)

(b)

Fig. 1. Current basis function $\boldsymbol{B}_{12}$ for (a) a curved parametric triangle and (b) a curved parametric quadrilateral.

The basis functions $\boldsymbol{B}_{ij}$ (Fig. 1(b)) associated with the corresponding edges are

$$\left.\begin{aligned} \boldsymbol{B}_{12} &= \frac{1}{4}\frac{(1-\eta)\boldsymbol{r}_\eta}{|\boldsymbol{r}_\xi \times \boldsymbol{r}_\eta|} & \boldsymbol{B}_{23} &= -\frac{1}{4}\frac{(1+\xi)\boldsymbol{r}_\xi}{|\boldsymbol{r}_\xi \times \boldsymbol{r}_\eta|}, \\ \boldsymbol{B}_{34} &= -\frac{1}{4}\frac{(1+\eta)\boldsymbol{r}_\eta}{|\boldsymbol{r}_\xi \times \boldsymbol{r}_\eta|} & \boldsymbol{B}_{41} &= \frac{1}{4}\frac{(1-\xi)\boldsymbol{r}_\xi}{|\boldsymbol{r}_\xi \times \boldsymbol{r}_\eta|}; \end{aligned}\right\} \quad (2)$$

with $\boldsymbol{r}_\xi = \partial\boldsymbol{r}/\partial\xi$, $\boldsymbol{r}_\eta = \partial\boldsymbol{r}/\partial\eta$, $-1 \leq \xi, \eta \leq 1$, and an arbitrary point $\boldsymbol{r}(\xi, \eta)$ on the quadrilateral is defined by $\boldsymbol{r}(\xi, \eta) = \sum_{i=1}^{8} \boldsymbol{r}_i N_i(\xi, \eta)$. For the definition of a quadratic parametric quadrilateral, eight nodal points $\boldsymbol{r}_i$ as well as their associated interpolation functions $N_i(\xi, \eta)$ $(1 \leq i \leq 8)$ are used [10]. In addition, the following relation holds: $\mathrm{div}_S \boldsymbol{B}_{ij} = -1/(4\ |\boldsymbol{r}_\xi \times \boldsymbol{r}_\eta|)$.

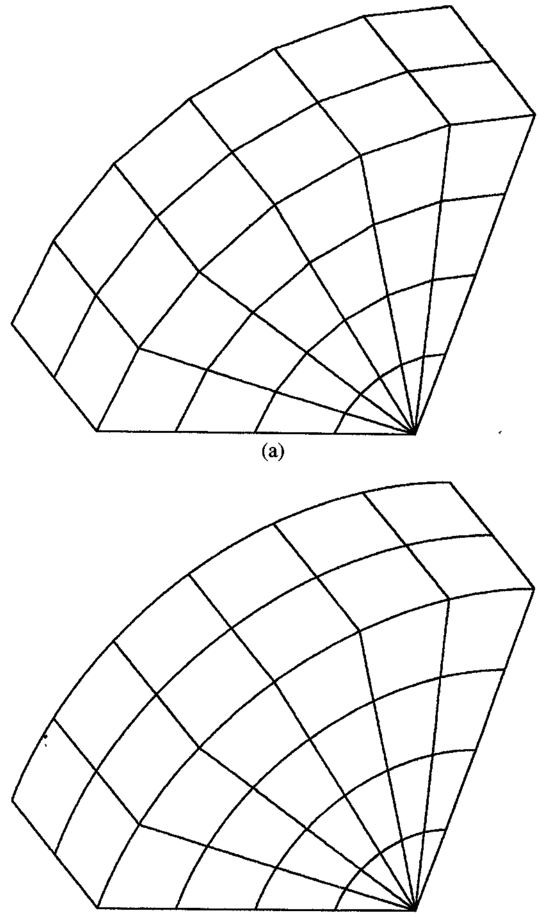

(a)

(b)

Fig. 2. Modeling one eighth of a circular cylindrical cavity by using 36 patches: (a) planar and (b) curved patches.

III. Numerical Results

The basis functions for curved parametric patches, both triangular and quadrilateral, have been applied in the MM solution of the EFIE for electromagnetic scattering and radiation from perfectly conducting surfaces of general shape. The techniques described in ([1], [2]) are used. A comparison between the numerical results by using these basis functions and exact or other numerical results confirmes the correctness and accuracy of both this method and its computer implementation.

It is well known that a numerical solution of an integral equation like the EFIE includes several steps, and all of them unavoidably introduce approximations. Obviously, the curved parametric patches discussed are superior in accurately modeling a given geometry to the conventional, planar ones. But does higher accuracy in the numerical solution necessarily result, if curved parametric patches are used instead of the planar ones?

For special applications, this question has partly been answered in [4], [5], and [7]. In this letter, cavities of different shape with a known exact solution have been chosen as examples, because a) there are more interior (cavity) problems with exact solutions than exterior ones and b) the accuracy of the numerical calculations can be judged by a single parameter, i.e., the resonance frequency. Both triangular and quadrilateral patches have been used.

TABLE I
CIRCULAR CYLINDRICAL CAVITY

No. of Patches	Type of Patches	$f_{H_{111}}$ (MHz) 173.74 217	$f_{E_{011}}$ (MHz) 188.77 165	$f_{H_{011}}$ (MHz) 236.41 801
9	curved	175.203 554	187.167 904	235.002 541
9	planar	176.834 364	189.477 153	239.116 101
36	curved	173.778 298	188.031 467	236.049 617
36	planar	174.181 587	188.597 427	237.077 181
81	curved	173.771 804	188.339 076	236.329 638
81	planar	173.946 843	188.582 164	236.782 408

TABLE II
SPHERICAL CAVITY

No. of Patches	Type of Patches	$f_{E_{101}}$ (MHz) 130.91 176	$f_{H_{101}}$ (MHz) 214.3961
25	curved	131.746 862	218.136 268
25	planar	134.785 882	191.683 343
36	curved	131.410 344	216.741 252
36	planar	133.493 664	220.058 887
81	curved	131.065 613	215.192 241
81	planar	131.979 495	216.640 183

Firstly, different resonance modes of a circular cylindrical cavity are considered. This cavity has a radius of 1 meter and a length of 1 meter as well. Due to the symmetry of the considered modes, only one eighth of the surface need be modeled. The different models with 36 planar and curved patches are depicted in Fig. 2. The dependence of the calculated resonance frequencies of the different modes on the type (curved or planar) and number of patches used are listed in Table I. Additionally, the exact resonance frequencies are also given.

It is evident from Table I that while for the H_{111} and H_{011} modes the numerically calculated resonance frequencies $f_{H_{111}}$ and $f_{H_{011}}$ are more accurate with curved patches than is the case with planar ones, for the E_{011} mode the reverse is true. The reason is not known yet. It should be remarked, however, that although higher accuracy in geometric modeling is achieved with curved patches, the errors due to the poor geometric modeling in case of planar patches and errors due to other approximations made in the numerical solution could still compensate each other under certain "lucky" circumstances.

The second example is a spherical cavity with a radius of 1 meter. Due to the symmetry of the resonance modes considered, again one eighth of the surface is taken for the calculation. The results are shown in Table II, together with the exact ones. In this example, the advantages of the curved parametric patches compared with the planar ones are clearly pronounced.

IV. CONCLUSION

Curved parametric triangular and quadrilateral basis functions were derived systematically from the edge elements of the FEM and have been used successfully in the MM solution of the EFIE. Numerical calculations of the resonance frequencies of cavities with curved walls and known exact solutions demonstrated that in most cases these basis functions are superior to their planar counterparts. Although some exceptions do exist, this kind of basis functions should preferably be used in the MM solution of integral equations.

In this letter, the curved parametric triangular and quadrilateral basis functions were constructed by combining the first order edge elements with quadratic triangles and quadrilaterals. Analogously, more basis functions can be derived from combinations of edge elements and triangles and quadrilaterals of different order. Higher order edge elements can be found, for example, in [12]–[14], while higher order triangles and quadrilaterals are described, for example, in [10]. Extrapolating the results achieved in ([4], [5]) by using node-based higher order basis functions, an application of higher order edge elements as basis functions in the EFIE should lead to a reduction in the number of patches used and an increase in accuracy.

The systematical application of first- and higher order basis functions in the numerical solution of different integral equations for electromagnetic scattering and radiation will be treated in a next step.

ACKNOWLEDGMENT

The authors thank the reviewers for pointing out reference [9] and for their constructive comments.

REFERENCES

[1] A. W. Glisson and D. R. Wilton, "Simple and efficient numerical methods for problems of electromagnetic radiation and scattering from surfaces," *IEEE Trans. Antennas Propagat.*, vol. AP–28, no. 5, pp. 593–603, 1980.

[2] S. Rao, D. R. Wilton, and A. W. Glisson, "Electromagnetic scattering by surfaces of arbitrary shape," *IEEE Trans. Antennas Propagat.*, vol. AP–30, no. 3, pp. 409–418, 1982.

[3] D. L. Knepp and J. Goldhirsh, "Numerical analysis of electromagnetic radiation properties of smooth conducting bodies of arbitrary shape," *IEEE Trans. Antennas Propagat.*, vol. AP–20, no. 5, pp. 383–388, 1972.

[4] M. Ingber and R. H. Ott, "An application of the boundary element method to the magnetic field integral equation," *IEEE Trans. Antennas Propagat.*, vol. 39, no. 5, pp. 606–611, 1991.

[5] H. Cam, S. Toutain, P. Gelin, and G. Landrac, "Study of a Fabry–Perot cavity in the microwave frequency range by the boundary element method," *IEEE Trans. Microwave Theory Tech.*, vol. 40, no. 2, pp. 298–304, Feb. 1992.

[6] A. Bossavit, "Whitney forms: A class of finite elements for three–dimensional computations in electromagnetism," *Proc. Inst. Elect. Eng., Pt. A*, vol. 135, no. 8, pp. 493–500, 1988.

[7] D. Wilkes and C.-C. Cha, "Method of moments solution with parametric curved triangular patches," in *Proc. IEEE Int. Symp. Antennas Propagat.*, 1991, pp. 1512–1515.

[8] S. Wandzura, "Electric current basis functions for curved surfaces," *Electromagn.*, vol. 12, no. 1, pp. 77–91, 1992.

[9] F. Dubois, "Discrete vector potential representation of a divergence–free vector field in three–dimensional domains: Numerical analysis of a model problem," *SIAM. J. Numer. Anal.*, vol. 27, no. 5, pp. 1103–1141, 1990.

[10] O. C. Zienkiewicz, *The Finite Element Method*, 3rd ed. London: McGraw–Hill Book Company, 1977.

[11] J. S. van Welij, "Calculation of eddy currents in terms of H on hexahedra," *IEEE Trans. Magn.*, vol. MAG–21, no. 6, pp. 2239–2241, 1985.

[12] C. W. Crowley, P. P. Silvester, and H. Hurwitz Jr., "Covariant projection elements for 3-D vector field problems," *IEEE Trans. Magn.*, vol. 24, no. 1, pp. 397–400, 1988.

[13] A. Kameari, "Calculation of transient 3-D eddy current using edge–elements," *IEEE Trans. Magn.*, vol. 26, no. 2, pp. 466–469, 1990.

[14] J. P. Webb and R. Miniowitz, "Analysis of 3-D microwave resonators using covariant–projection elements," *IEEE Trans. Microwave Theory Tech.*, vol. 39, no. 11, pp. 1895–1899, Nov. 1991.